Automatic Determination of Acoustic Plate Source-Detector Separation from One Waveform

Stephen D. Holland[1] and Wolfgang Sachse[2]

[1]Center for Nondestructive Evaluation, Iowa State University, Ames, IA 50011
[2]Department of Theoretical and Applied Mechanics, Cornell University, Ithaca, NY 14853

Corresponding author:

Stephen D. Holland
Iowa State University
ASC II
1915 Scholl Road
Ames, IA 50011
sdh4@cornell.edu
515-294-8659

Abstract

We discuss an automated procedure for determining the separation between a transient acoustic source and a detector on a plate. We use a time-estimation algorithm based on the assumption that the detected signal is represented by a small finite number of discrete band-limited impulses. This is carried out using the MUSIC (MUltiple SIgnal Classification) algorithm in time-estimation mode to automatically estimate both the first arrival time of the lowest order antisymmetric (A_0) mode and the arrival time of the Rayleigh wave. Using the material and geometric properties of the plate and these two arrival times we calculate the distance to the source. This technique allows the automatic determination of source-receiver separation from a single transient waveform.

1 Introduction

Acoustic emission (AE) signals are the transient elastic waves emitted from a localized change of stress or strain in a material. As such, AE signals are emitted when deformation and failure processes occur in a specimen. Much research over the last four decades has focused on the processing of AE waveforms to recover the location and the characteristics of the acoustic source. AE processing has progressed from event counting to source location to model-based source characterization. AE analysis parallels closely the equivalent seismic problem of finding the epicenter of an earthquake [1]. Today, an experienced seismologist can usually locate a major earthquake accurately with a single seismogram. The different arrival times – of pressure, shear, Rayleigh, and mode-converted waves – can be used to accurately estimate the distance, and knowledge of likely earthquake zones is usually sufficient to determine the azimuth. Similarly, an experienced AE researcher or technician can identify multiple arrivals within an AE waveform and thereby determine the distance to the source.

In conventional AE waveform processing, a single arrival time is recorded for each transducer. Solving the source location problem in n-dimensional space requires at least $n + 1$ transducers because the event source time t_0 is unknown. With the large number of sensors in conventional AE systems, obtaining $n + 1$ signals is generally not a problem, but due to the dispersive nature of wave propagation in thin plates, the wave arrivals are not well defined. If two precise arrival times can be obtained from each transducer then that can improve the solution of the source location problem. Alternatively, transducer spacing can be widened, providing coverage equivalent to single arrival AE, but with fewer sensors. There are several established methods for extracting multiple arrival times from AE signals in two-dimensional plates. These exploit the dispersion of Rayleigh-Lamb guided modes to identify distinct arrivals as functions of time. We note in particular a patent [2] which describes a procedure for extracting multiple arrival times from a single AE waveform, and the work of Gorman [3], who discusses the utility of Lamb wave theory for detailed analysis of synthetic AE waveforms in plates.

Time-frequency representations have been used for Lamb wave analysis since the late 1990's. Prosser et al.[4] applied the Wigner-Ville distribution in the context of AE waveform processing to analyze simulated waveforms from an aluminum plate and experimental waveforms from a model source (pencil lead fracture) on a composite plate. Our own previous publication describes an explicit method for determining two arrival times from synthetic or experimental data based on the Wigner-Ville distribution [5]. Niethammer et al. [6] provides a detailed comparison of the characteristics and relative merits of different time-frequency representations, including the Fourier spectrogram, wavelet scalogram, Wigner-Ville distribution, and Hilbert spectrum. Hurlebaus et al. [7] introduced and Benz et al. [8] refined an autonomous correlation-based technique for locating a notch based on time-frequency analysis of notch-scattered laser pulse-generated Lamb modes.

In this paper we describe an automatic method for extracting a second arrival time from the waveform detected by each transducer on a thin two-dimensional plate. Given two arrival times t_1 and t_2, the material properties, and group velocities V_{g1} and V_{g2} calculated from Lamb wave theory, the source distance d and event time t_0 can be directly evaluated:

$$d = V_{g1} V_{g2} \frac{t_2 - t_1}{V_{g1} - V_{g2}} \tag{1}$$

and

$$t_0 = \frac{V_{g1} t_1 - V_{g2} t_2}{V_{g1} - V_{g2}}. \tag{2}$$

The method we describe below works autonomously and does not require manual intervention other than initial parameter adjustment. It relies upon time-frequency analysis using the MUSIC (MUltiple SIgnal Classification) spectrum and root-MUSIC frequency identification algorithm [9] to measure distinct and physically meaningful arrival times for each signal in two different frequency bands. Elastic wave detection is with a miniature piezoelectric transducer. We use the fracture of a glass capillary (step unloading) as a model AE source and a glass plate as a propagating medium. Glass was chosen because it is a uniform, isotropic, well-characterized, low-attenuation medium, and not for any specific application. Real AE sources might be of lower amplitude and of different type than the capillary fracture signal leading to lower signal-to-noise ratio (SNR). Engineering metals such as aluminum or steel would behave similarly to glass, but with higher attenuation and the concomitant reduction in SNR at large distances. The algorithm we describe assumes that only an isolated source event is detected in each recorded waveform.

2 Time-frequency analysis of waveforms

Figure 1 shows the measurement geometry and a sample waveform (2000 samples, $f_s = 10$ MHz) generated by the fracture of a glass capillary on a glass plate of thickness $h = 0.4$ in (10.2 mm), with a source-receiver separation $d = 28$ in (711 mm, or $70h$). When acoustic waves propagate in plates, only a discrete set of Rayleigh-Lamb modes propagate. These wave modes are dispersive, in the sense that their wavespeeds are frequency dependent, so that a propagating pulse distorts and disperses as it propagates along the plate. The dispersion relations of the modes can be calculated from theory given the material parameters [10], the group velocities $\partial\omega/\partial k$ as functions of frequency are easily calculated from the

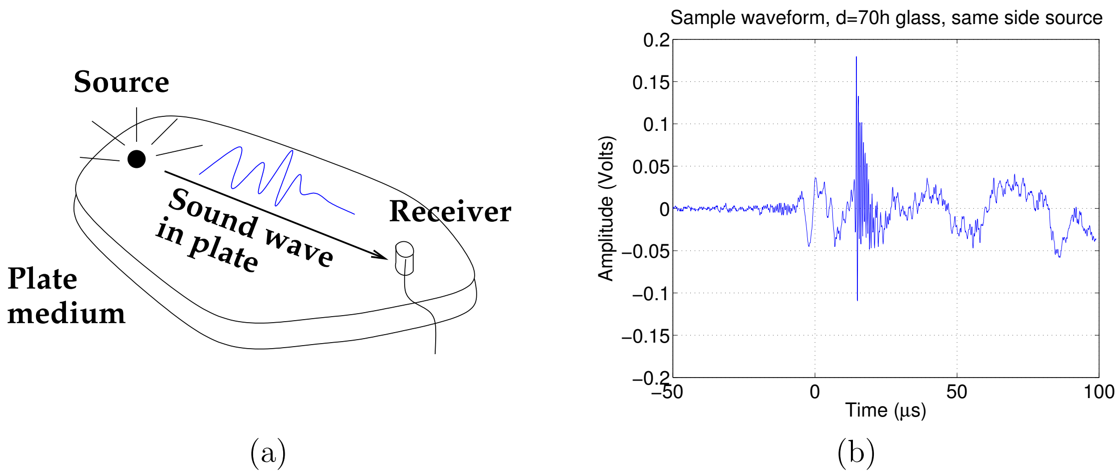

Fig. 1. (a) Measurement geometry (b) sample waveform (distance d=70 thicknesses of $h = 0.4$ in thick glass)

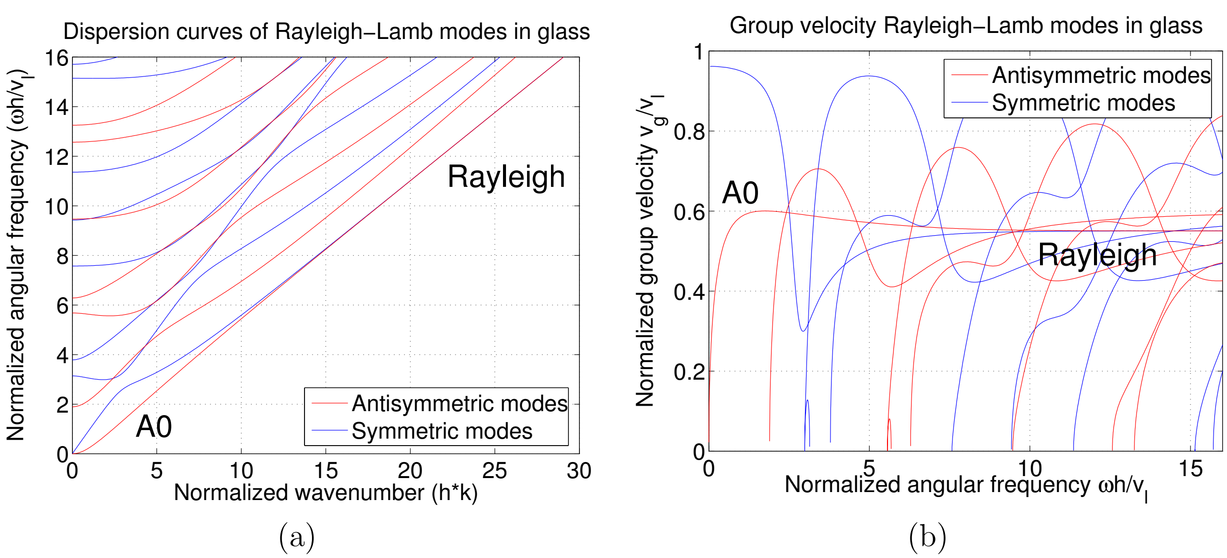

Fig. 2. (a) Dispersion relations for glass (b) Group velocity curves for glass

dispersion relations. Fig. 2 shows the dispersion relations and corresponding group velocities for a glass plate. The measured impulse response after propagation will consist of a discrete pattern of arrivals at times inversely proportional to group velocity $T = d/V_g$. We will exploit the discrete nature of these arrivals by analyzing them with a discrete model and MUSIC.

3 MUSIC

The MUSIC algorithm was originally developed for the estimation of the direction of an electromagnetic signal impinging on an array of antennas [9]. It is an algorithm for estimation of the frequency of a signal in a noisy environment. MUSIC has the advantage of computational efficiency; the computation time for all the calculations described herein is just a few seconds on a modern 2 GHz PC. While MUSIC is, by now, a textbook algorithm (e.g. [11]), we will discuss it in some detail, both because its use is relatively rare in the acoustics community and because we are using it for time-estimation instead of frequency-estimation.

The MUSIC algorithm assumes that the signal to be measured can be modeled as a sum of k harmonic waves plus additive white Gaussian noise $N(t)$. Given the stationary model,

$$x(t) = \sum_{i=1}^{k} A_i \exp(j2\pi f_i t) \quad + \quad N(t), \tag{3}$$

MUSIC generates a spectral analysis with maxima at or near the frequencies f_i from the time-samples of $x(t)$. What is needed is a simple and effective method for finding those frequencies from the samples. The root-MUSIC algorithm accomplishes this by transforming the frequency estimation problem to a polynomial root finding problem, which is easily solved. MUSIC is useful for frequency-estimation because it provides higher resolution with less input than Fourier analysis.

We will apply MUSIC to time-estimation by performing frequency-estimation on the Fourier transform of our measured waveforms, thereby measuring arrival times instead of frequencies. We assume that a waveform is a sum of k discrete impulses plus noise,

$$x(t) = \sum_{i=1}^{k} A_i \delta(t - t_i) \quad + \quad N(t), \tag{4}$$

where t_i is the time of the i-th impulse, or equivalently in the frequency domain,

$$X(f) = \sum_{i=1}^{k} A_i \exp(-j2\pi f t_i) \quad + \quad N(f). \tag{5}$$

In the frequency domain we have a sum of harmonic waves, analogous to the time-domain MUSIC model of Eq. 3. Measuring the periodicity of these harmonic waves will give us the arrival times of the impulses. By operating on this model, MUSIC takes advantage of *a priori* knowledge about the signal being analyzed. In contrast to Fourier analysis which assumes the signal to be an infinite sum of harmonic waves, MUSIC analysis assumes the signal to consist of a sum of a small number of discrete harmonic waves. By exploiting this *a priori* knowledge, MUSIC analysis is able to determine the frequency of those frequency-domain harmonic waves, and hence the times of the impulses, more precisely than possible with Fourier transform-based techniques. As will be discussed below, this is particularly suitable to the study of guided modes, where waves can only propagate at particular combinations of frequency and spatial wavenumber.

We start by obtaining N time samples of $x(t)$, where f_s is the sampling frequency,

$$x[n] = x\left(\frac{n}{f_s}\right), \quad n = 0, 1, \ldots (N-1). \tag{6}$$

The first and last 25 μs of these samples have been windowed with a raised cosine to avoid a transient between $n = N-1$ and $n = 0$. The discrete Fourier transform (DFT) transforms these samples into the frequency domain, and yields

$$X[\mathfrak{f}] = \sum_n x[n] e^{-j2\pi n\mathfrak{f}/N}, \mathfrak{f} = 0, 1, \ldots (N-1). \tag{7}$$

$X[\mathfrak{f}]$ is a complex, discrete frequency domain spectrum consisting of N frequency-domain samples. The discretized frequency $\mathfrak{f}$ has integer values and can be multiplied by (f_s/N) to obtain the actual frequency in Hz. We will look at the frequency domain samples $X[\mathfrak{f}]$ in groups of M ($<< N$). By using only a subset of the frequency-domain samples, we are able to determine an arrival time corresponding to a limited frequency range, independent of arrivals in other frequency regions. We next define the covariance length L, which is the number of frequency-domain samples over which we analyze for correlations. MUSIC requires the $L \times L$ covariance matrix $R = EXX^{\mathrm{T}}$, where E is the expectation operator and X is a set of L frequency-domain samples. The estimate $\hat{R}$ of the covariance matrix R is constructed in Toeplitz form from the $(2L-1)$ central samples of the autocorrelation of the M samples of $X[\mathfrak{f}]$. Each element on the i-th diagonal of $\hat{R}$ is set to the i-th element of the autocorrelation.

To perform MUSIC time-estimation, we construct the eigen decomposition of R,

$$U\Lambda U^{\mathrm{T}} = R, \tag{8}$$

where U is the matrix of eigenvectors and Λ is diagonal and contains the eigenvalues. It stands to reason that if $X[\mathfrak{f}]$ comes from a sum of k harmonic waves plus noise, we would expect the eigenvectors of R (columns of U) corresponding to the largest k eigenvalues (diagonal elements of Λ) to be related to those k harmonic waves and, further, the remaining $L-k$ eigenvectors to be related to the noise. In MUSIC and root-MUSIC, we discard the 'signal' eigenvectors and focus on the 'noise' eigenvectors. These eigenvectors contain little energy at the particular frequencies of the k harmonic waves because energy at those frequencies is contained in the 'signal' eigenvectors.

We create a composite waveform $W[\mathfrak{f}]$ by summing the autocorrelations of the $L-k$ noise eigenvectors. As the noise eigenvectors have little energy at the signal frequencies, nor will the sum of their autocorrelations. The MUSIC time spectrum, $C(t)$, is the reciprocal of the Fourier transform of $W[\mathfrak{f}]$,

$$C(t) = \frac{1}{\sum_{\mathfrak{f}} W[\mathfrak{f}] e^{jt2\pi\mathfrak{f}f_s/N)}}. \tag{9}$$

The maxima in the MUSIC time spectrum $C(t)$, the zeros in the spectrum of W, are the estimated arrival times t_i of the k impulses. (Recall here that $\mathfrak{f}$ is discrete and has integer values so the quantity $\mathfrak{f}f_s/N$ is the actual frequency in Hz.)

To precisely identify these times, we must find the k maxima of the MUSIC spectrum or alternatively the spectral zeros of W. The 'root-MUSIC' algorithm transforms this problem into one of finding the roots of a polynomial. We want to find the specific times t_i such that the inner product of $W[\mathfrak{f}]$ with $e^{jt_i 2\pi\mathfrak{f}f_s/N}$ is zero, or equivalently

$$\sum_{\mathfrak{f}} W[\mathfrak{f}] e^{(j2\pi t_i f_s/N)\mathfrak{f}} = 0. \tag{10}$$

If $z = e^{j2\pi t_i f_s/N}$, then Eq. 10 is equivalent to

$$\sum_{\mathfrak{f}} W[\mathfrak{f}] z^{\mathfrak{f}} = 0, \tag{11}$$

a polynomial in z, which is the z-transform of $W[\mathfrak{f}]$. We can find z and hence $e^{jt_i 2\pi f_s/N}$ by finding the zeros of this polynomial. The arrival times t_i can then be calculated from those zeros of the polynomial which lie on the unit circle in the complex plane

$$t_i = \frac{N}{2\pi f_s} \text{imag}(\ln\ z_i). \tag{12}$$

Eq. 12 gives the estimated arrival times t_i of impulses present in the original signal $x(t)$.

4 Procedure

The MUSIC algorithm can be used to autonomously and automatically extract two arrival times from measured waveforms obtained from a simulated AE step source. We apply MUSIC, as discussed above, to the Fourier transform of a measured Rayleigh-Lamb waveform. We can create a MUSIC spectrogram by automatically sliding the frequency range window used for time-estimation and thereby determining the arrival times as functions of frequency. Fig. 3a shows calculated arrival time curves d/V_g of Lamb modes for 711-mm propagation of an impulse source in 10.2-mm thick glass. Fig. 3b shows a MUSIC time-estimation spectrogram of the corresponding experimentally measured waveform of Fig. 1b ($f_s = 10$ MHz, $N = 2000$ samples). The MUSIC spectrogram shows estimated arrival time as a function of the center of the frequency range used for estimation, with parameters of $M = 48$ frequency-domain samples, equivalent to 235 kHz, and correlation length $L = 24$ samples, equivalent to 115 kHz. Since MUSIC requires knowledge of the number of frequencies to be estimated,

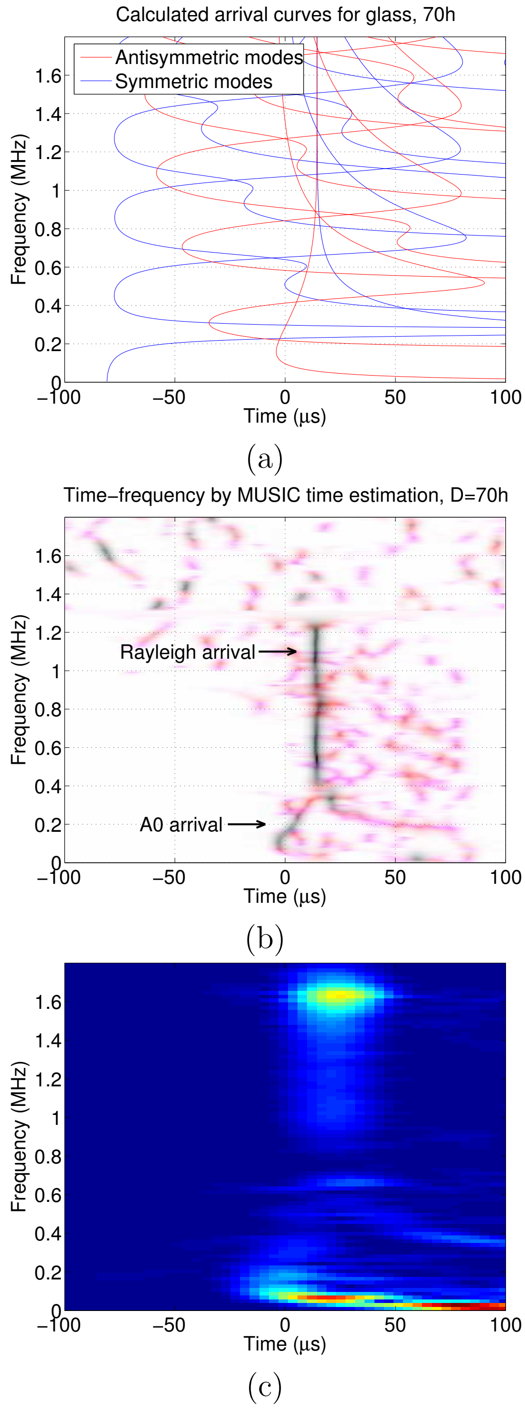

Fig. 3. (a) Calculated arrival times (excitation time t=-208.3μs) (b) MUSIC spectrogram (c) Fourier spectrogram

we have added together normalized spectrograms assuming the number of signals k to be one, three, and six, so that the dominant arrivals are shown darker. Fig. 3c shows, a Fourier spectrogram calculated from the same data as that shown in Fig 3b. The spectrogram in Fig. 3c was generated with a 256 point Hamming window and has not been enhanced with contrast enhancement or any reassignment algorithm. This should not be considered a comparison with a state-of-the-art time-frequency representation, but as illustrative of some of the differences between a MUSIC spectrogram and a Fourier spectrogram. For example, the MUSIC time-estimation spectrogram does not in any way represent the energy of the signal as does the Fourier spectrogram, but it does show much finer resolution than the unprocessed Fourier spectrogram.

In the experiments carried out here we have found that two wave modes in particular are readily identifiable in the time-estimation MUSIC. The first A0 (lowest order asymmetric) arrival and the Rayleigh arrival (high frequency combination of lowest order asymmetric and lowest order symmetric) are in this case found to be the highest MUSIC-spectrum amplitude arrivals in their corresponding frequency bands, which can be determined by calculation from Lamb wave theory and optimized by using measured waveforms from a variety of source-receiver separations. These are the arrivals shown darkest in Fig. 3b at the selected frequency ranges of 90 to 330 kHz and .8 to 1.2 MHz respectively. In order for our algorithm for extracting two arrival times to work, these two modes must be dominant within their respective frequency bands. The presence of other modes will not necessarily inhibit determination of the arrival times, provided that other modal arrivals are weaker in amplitude in the selected frequency bands. A key advantage of using MUSIC is that with Eq. 12 it gives a direct ('root-MUSIC') estimation of the wave mode arrival times. Since the A0 and Rayleigh arrivals are the largest amplitude arrivals in their respective frequency bands, application of root-MUSIC to the windowed frequency-domain waveform will give the A0 and Rayleigh arrival times. Fig. 4 shows these estimated arrivals as vertical lines. The parameters for the root-MUSIC algorithm were window widths of $M = 48$ samples (235 kHz) and $M = 80$ samples (395 kHz) for the A0 and Rayleigh modes respectively, and autocorrelation lengths of $L = 16$ samples (75 kHz) and $L = 30$ samples (145 kHz) respectively for the two modes. These values are shown as brackets around these modes in Fig. 4. These values were the only manually selected parameters to the otherwise autonomously generated results to be described next.

Once the A0 and Rayleigh arrival times have been determined, then the distance to the source can be evaluated according to Eq. 1 from the known group velocities $V_{g1} = 3.48$ mm/μs and $V_{g2} = 3.20$ mm/μs of the A0 and Rayleigh modes at those frequencies. The excitation time t_0 can similarly be calculated from Eq. 2. This procedure is inherently limited to thin plate geometries where Lamb wave theory is applicable, but is is otherwise independent of scale provided the wave propagation distance is many times the thickness.

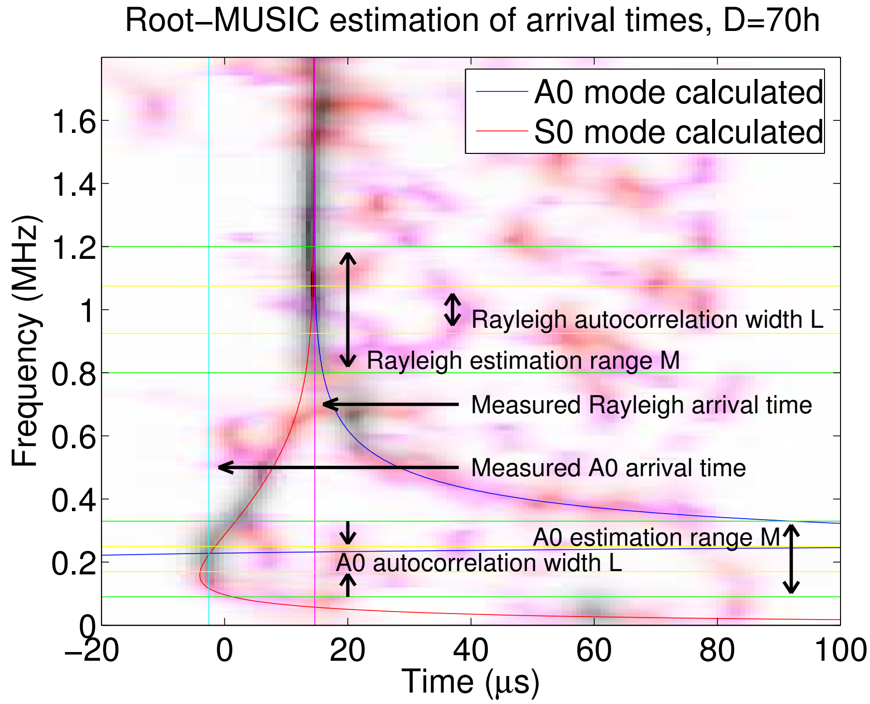

Fig. 4. Determination of arrival times with root-MUSIC.

5 Results and Discussion

With the calculation parameters fixed at the values specified in section 4, the automatic determination procedure was tested on waveforms detected by a small-aperture transducer from a simulated AE source over a range of source-receiver separations. Seventy-two waveforms were generated with glass-capillary-fracture step excitation on a $h = 0.4$ in (10.2 mm) thick glass plate and recorded with a 2-mm aperture piezoelectric transducer at distances ranging from $5h$ through $70h$, with the source on the same side of the sample as the detector, and at distances ranging from $20h$ through $70h$ with the source on the opposite side. The MUSIC algorithm was applied to each of these waveforms to estimate the source-receiver separation. Fig. 5a shows the measured separations $\hat{d}$ as as function of actual distance d. The relative error $((\hat{d} - d)/d)$ in percent is given in Fig. 5b. Excluded from Fig. 5b are the measurements for opposite-side sources at $d = 20h$ and measurements for same-side sources at $d = 5h$, because the method failed for these situations, in the sense that the relative error exceeded 100%. No data was recorded for opposite-side sources at $d < 20h$ or for same-side sources at $d < 5h$. Error bars in Fig. 5b indicate the peak error over 100 root-MUSIC calculations with the L and M parameters randomly varied by ± 8 samples (± 35 kHz), except in the A0 estimation in which L varied by ± 2 samples (± 5 kHz). It is clear from Fig. 5 that in this demonstration experiment the source-receiver separation was effectively measured at separations beyond 5h for a same-side source and beyond $20h$ for an opposite side source.

The method relies on measuring the time delay between the arrivals of the A0 and

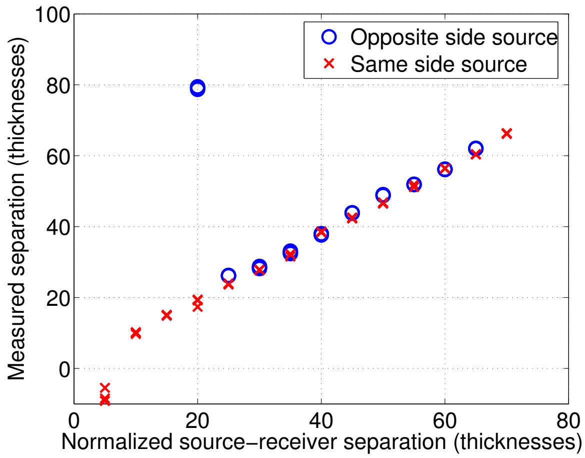

(a)

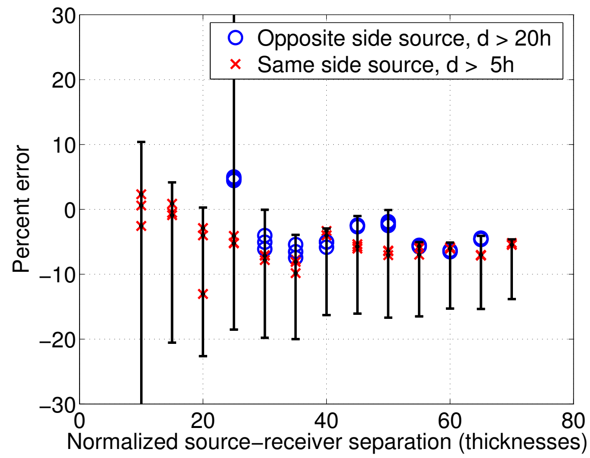

(b)

Fig. 5. (a) Source-receiver separation measured automatically from a single waveform with MUSIC as a function of actual separation. (b) Percent error in automatic thickness measurement as function of separation. The opposite side data points at d=20h and same side data points at d=5h have relative error $> 100\%$ and are not shown in (b).

Rayleigh wave modes, and therefore requires a substantial separation because otherwise the delay will be very small and thus a small absolute error will translate into a large relative error. This can be observed as a widening of the error bars in Fig. 5b for shorter distances with the largest relative errors at the shortest distances. We also note that same-side measurements are successful at smaller separations than measurements on the opposite side. This is a consequence of this method's reliance on the Rayleigh mode arrival. The Rayleigh mode is primarily a surface wave and is most effectively generated by a source on the same side of the sample as the detector. Spectrograms of waveforms at short distances show the presence of higher order modes, and these can also cause interference to the MUSIC algorithm when their amplitude is large relative to the Rayleigh mode amplitude. Finally, it is clear from the figure that at large separations there is a bias of around -5% in the results and about -10% in the error bars. Our calculation of the distance from the arrival time difference of the two dominant modes assumes the shortest time/highest velocity for the A0 mode. However, in practice the A0 arrival is very narrowband in frequency. Therefore the measured arrival time will not be the shortest time, but an average time over the specified frequency band, hence the bias. The larger estimation ranges used in the error bar calculations exacerbate this effect and hence the bias appears larger in the error bars. Recognizing these facts, the bias could be trivially subtracted out.

Numerical experiments involving adding white Gaussian noise to the detected waveforms have indicated how this algorithm might perform on signals from weaker sources or signals propagating in more attenuative materials. In particular, it was observed that this method gave reliable and accurate results from the measurements reported above, as long as the signal-to-noise ratio was not reduced below approximately 3.0. With lower signal-to-noise ratios this method yielded nonsense results, with very large and usually obvious errors such as negative source-receiver separations or relative errors exceeding 100%). As the signal-to-noise ratio is reduced on a single waveform, only a slight (typ. $< 20\%$) increase in estimation error is observed until a point is reached when the algorithm entirely misidentifies one of the wave arrivals, which leads to a nonsensical result.

6 Conclusions

We have demonstrated the utility of the MUSIC algorithm and MUSIC analysis in a time-estimation mode for analyzing waves that have propagated in thin plates. We have described a specific method for autonomously extracting two arrival times from a single waveform. In the example shown the method extracted the arrival times of the A0 and Rayleigh wave modes. These two arrival times have then been used to calculate both the source-receiver separation and the excitation time in a plate of two-dimensional geometry.

The method has been demonstrated on one test series of seventy-two capillary-fracture-source waveforms with source-receiver separations ranging from $5h$ to $70h$. The method correctly and autonomously determined the source-receiver separation for same-side excitation starting at $10h$ and for opposite side excitation starting at $25h$. From this demonstration experiment, it is clear that when this method is implemented in practice, limits of applicability must be established under the conditions for which it is to be used to locate sources of acoustic emission in a thin plate.

7 Acknowledgments

The authors would like to thank Wei Zou and Tadej Kosel for providing the experimental waveforms for analysis. This work made use of the computing facility of the Cornell Center for Materials Research (CCMR) with support from the National Science Foundation Materials Research Science and Engineering Centers (MRSEC) program (DMR-0079992).

References

[1] Y.H. Pao, "Theory of Acoustic Emission", in *Elastic Waves and Non-destructive Testing of Materials*, Y.H. Pao, Ed., AMD-Vol. 29, ASME, New York (1978), pp. 107-128.

[2] W. Sachse and S. Sancar, Acoustic Emission Source Location on Plate-like Structures using a Small Array of Transducers. U. S. Patent No. 4,592,034 Filed: November 15, 1982; Issued: May 27, 1986.

[3] M. R. Gorman, Plate wave acoustic emission, J. Acoust. Soc. Am. **90**(1) 358-364 (1991)

[4] W. H. Prosser, M. D. Seale, and B. T. Smith, Time frequency analysis of the dispersion of Lamb mode, J. Acoust. Soc. Am. **105**(5) 2669-2676 (1999).

[5] S. Holland, T. Kosel, R. Weaver, and W. Sachse, Determination of plate source, detector separation from one signal, Ultrasonics **38** 620-623 (2000).

[6] M. Niethammer, L. J. Jacobs, J. Qu, and J. Jarzynski, Time frequency representations of Lamb waves, J. Acoust. Soc. Am. **109**(5) 1841-1847 (2000).

[7] S. Hurlebaus, M. Niethammer, L. J. Jacobs, C. Valle, Automated methodology to locate notches with Lamb waves, Acoustics Res. Lett. Online **2**(4) 97-102 (2001).

[8] R. Benz, M. Niethammer, S. Hurlebaus, L. J. Jacobs, Localization of notches with Lamb waves, J. Acoust. Soc. Am **114**(2) 677-685 (2003).

[9] R.O. Schmidt. Multiple Emitter Location and Signal Parameters Estimation, IEEE Trans. Antenna Propag. **34**(3) 276-280 (1986).

[10] R. L. Weaver and Y. H. Pao, Axisymmetric elastic waves excited by a point source in a plate, Transactions of the ASME. J. Appl. Mech., **49**(4) 821-836 (1982).

[11] P. Stoica and R. L. Moses, *Introduction to Spectral Analysis*, Prentice Hall, Upper Saddle River, NJ (1997), pp 155-160.